*Journal of Low Temperature Physics, Vol. 134, Nos. 5/6, March 2004 (© 2004)*

# Effect of $^3$He on Third Sound Attenuation in Thick $^4$He Films

**K. Penanen,[1,2] J. A. Hoffmann,[1,3] J. C. Davis,[3] and R. E. Packard[1]**

[1] *Physics Department, University of California at Berkeley, Berkeley, California 94720, USA*
E-mail: Konstantin.Penanen@jpl.nasa.gov
[2] *Jet Propulsion Laboratory, California Institute of Technology, Pasadena, California 91109, USA*
[3] *LASSP, Physics Department, Cornell University, Ithaca, New York 14853, USA*

(Received August 24, 2003; revised November 4, 2003)

*We have performed measurements of third sound attenuation in thick films of superfluid $^4$He in the presence of small amounts of $^3$He. The attenuation due to $^3$He appears to depend linearly on the number density of $^3$He atoms in the film. We discuss the results in context of a recently proposed mechanism where the attenuation is caused by the interaction of the excitations in helium with the trapped vortices.*

***KEY WORDS***: third sound; helium film; quantized vortices.

Films of $^4$He provide an example of a superfluid in a restricted geometry. Unhampered by viscosity, the superfluid component is free to move along the substrate surface. This system allows propagation of third sound,[1,2] a long wavelength hydrodynamic mode similar to gravity waves in shallow water. Although persistent currents exist in the films,[3,4] time-varying flow such as third sound is attenuated by mechanisms that are still not well understood. Liquid helium is exceptionally free of contaminants, which freeze out at higher temperatures. However, the presence of the $^3$He isotope, even in small amounts, alters some of the transport properties beyond what one would expect by assuming that $^3$He simply enhances the normal component of a homogeneous superfluid. For example, in persistent-current decay measurements,[5] the rate of decay increases in the presence of $^3$He. Also, small amounts of $^3$He reduce the thermal conductivity in superfluid films adsorbed on strips of Mylar.[6] Similarly, trace amounts of $^3$He reduce the rate at which the superfluid film flow replenishes a heated region on a silicon substrate.[7]



0022-2291/04/0300-1069/0 © 2004 Plenum Publishing Corporation

In this paper we report how small amounts of $^3$He affect the attenuation of third sound in a thick helium film. We find that the third sound attenuation is proportional to the $^3$He fraction but the proportionality factor can be reset by traversing the superfluid transition temperature. This suggests that the attenuation is due to trapped remnant vortices which, as was first shown by Ellis *et al.*,[8] densely populate helium films. The periodically swaying trapped vortices interact with the $^3$He background and dissipate the energy in the third sound.

We study third sound in a thick ($\sim$300 Angstrom) saturated film adsorbed on the surfaces of a circular resonator. The resonator is placed inside of a temperature-controlled can (of approximately 200cc internal volume), which is connected via a weak thermal link to the $^3$He pot of a sorption-pumped refrigerator. Temperature control of $\sim 0.3$ mK is maintained, while the temperature is varied between the base temperature of the refrigerator of $\sim 0.25$ K and the bulk superfluid transition at 2.17 K. The cell is filled through a $^3$He-actuated, superfluid-leak-tight valve, which remains sealed after helium is added. Both $^4$He and $^3$He are metered into a container of known volume and introduced into the cold cell at $T \approx 1.3$ K. The concentration numbers we use refer to the molar concentration of $^3$He in the room temperature mixture.

Both the excitation and detection of the third sound are performed capacitively.[9] Helium films cover the surfaces of a polished brass pedestal, which forms the bottom surface of the resonator, and of a glass flat, which forms the top surface. The glass flat is patterned with evaporated gold film ($\sim$200 nm thick) to produce four conducting quadrants composing the drive and detector capacitor plates. To reduce the capacitive cross-talk, the quadrants are separated by a grounded cross-shaped electrode. The active area of each quadrant is 1.63 cm$^2$, and the spacing between the quadrants and the pedestal, calculated from the measured capacitance between the quadrants and the pedestal, is between 38 and 60 μm. To avoid capillary filling of the space between the pedestal and the glass, the support structure of the glass holder is separated from the pedestal radially by $\sim 1.5$ mm, which is larger than the helium capillary length.

We find that the resonator exhibits normal modes that we identify closely with the Bessel function modes of a drum head. Such modes would appear if the tangential component of the superfluid velocity vanishes at the edge. This condition is equivalent to fixed boundary conditions for the film height variation at the edge. Why these boundary conditions dominate is not clear. Several resonant modes were detected and identified. These modes correspond to resonances on either the glass flat or the brass substrate. In this work we report attenuation of a single mode on the glass flat, which is most efficiently excited and detected by our electrode configuration.

This is the anti-symmetric Bessel mode of the first kind with $m = 1$, $n = 1$, typically at resonant frequency $f \approx 26$ Hz. The resonance is excited with one of the quadrants and is efficiently detected at the diagonally opposite quadrant. We drive the mode with a sinusoidal drive signal of typical amplitude $\sim 5$ V. Electrostrictive force, which is proportional to the square of the applied voltage, excites the mode of interest. The detection quadrant capacitor, biased to $\sim 100$ V DC through a $10^{12}\,\Omega$ resistor, is connected through a blocking capacitor to a low noise voltage preamplifier[10] and to the input of a lock-in amplifier[11] which is referenced to the second harmonic of the drive signal. The drive frequency is swept across the resonant response while frequency, in-phase, and in-quadrature responses are recorded. The spectrum, which consists of several damped simple harmonic oscillator modes, then undergoes an analysis procedure in which the amplitudes, positions and the quality factors of the mode of interest and nearby modes are simultaneously fit to the real and the imaginary components of the response. Variation in the peak position corresponds to the change in third sound wave speed of propagation, while the peak width represents the dissipation. We calculate the attenuation from the resonance condition, $\omega = \frac{c_3 Z_{1,1}}{R}$ and the relation between the quality factor of a resonant mode and the attenuation, $\alpha = \frac{\omega}{2Qc_3} = \frac{Z_{1,1}}{2RQ}$. Here $c_3$ is the third sound velocity, $Z_{1,1} \approx 3.83$ is the first zero of the Bessel function, $J_1(x)$, $R$ is the radius of the glass flat and $Q$ is the quality factor of the resonant mode. Because the third sound velocity varies with temperature due to the changes in superfluid density, the dependence of the attenuation on frequency is implicit through the change of the resonant frequency with temperature. It is, however, of no significance in further discussion, since the effects we describe manifest themselves below $T \approx 1.5$ K, where the third sound velocity changes are small.

Figure 1 shows the temperature dependence of the attenuation for the $m = 1$, $n = 1$ mode for mixtures with two different amounts of $^3$He in the cell. The attenuation is reproducible if the temperature in the cell is varied slowly and if the temperature is not raised above the superfluid transition. However, as shown in the figure, cycling the sample through $T_\lambda$ sets the system on a new attenuation curve. This strongly suggests that the film typically exists in a metastable state which can be modified by thermal cycling though $T_\lambda$.

Note that the attenuation first decreases as temperature is lowered from 2 to $\sim 1.3$ K as one might expect from attenuation mechanisms arising from vapor recondensation,[12,13] thermal conductivity through the substrate, or vortex-normal fluid interaction.[14] However, as the temperature is lowered further, the attenuation reaches minimum values and then begins to *increase*. The minimum attenuation and the temperature at which the minimum occurs depend on the amount of $^3$He in the cell.

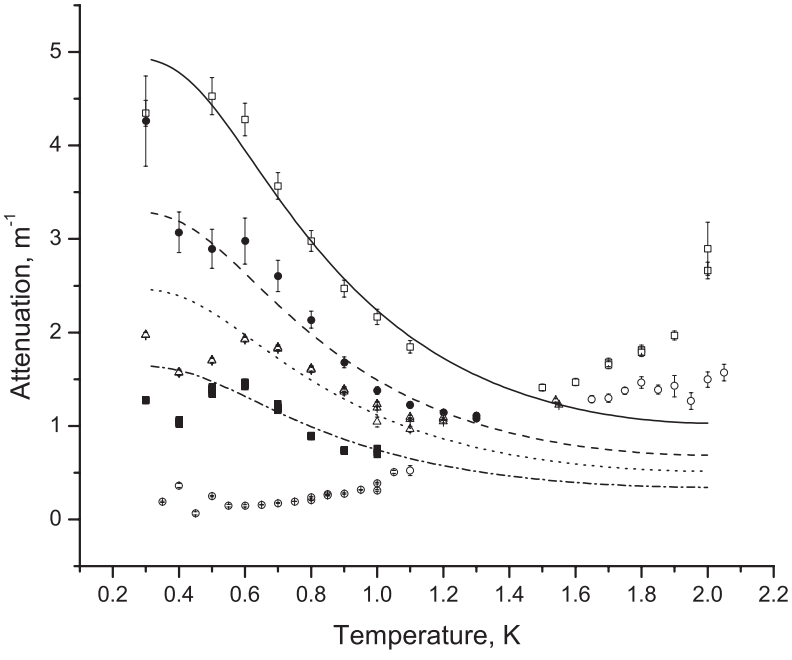


Fig. 1. Attenuation vs. temperature for helium mixtures containing 330 ppm (solid squares and open up triangles) and 660 ppm (solid circles and open squares) $^3$He. Error bars represent fit quality for individual attenuation measurements. Attenuation is reproducible unless the film state is reset by warming above $T_\lambda$. Lines through the data represent a model in which the attenuation is proportional to the $^3$He content *in the film*. The model multiplier $\beta$ (proportional to the number density of remnant trapped vortices in the model described in the text) is 7500 m$^{-1}$ for the solid and short-dash lines, and 5000 for the short-dash and dash-dot lines. A set of attenuation measurements for helium with no added $^3$He is shown by open circles. In these measurements, attenuation was calculated from free decay of oscillations caused by a tone burst. The data below $\sim$1.3 K is obtained with the adsorption refrigerator running; the data above 1.5 K is obtained with 1 K pot providing cooling through the exchange gas in the adsorption refrigerator subsystem. The data in the intermediate regime was not taken in most data sets due to severely shortened holding times of the adsorption refrigerator.

As the temperature is lowered, the concentration of $^3$He in the film increases due to condensation from the vapor. This concentration can be calculated from chemical potential equilibrium between the vapor and the liquid phases. We then can compare the temperature dependence of the $^3$He concentration in the film and the attenuation.

To calculate the molar concentration of $^3$He in the liquid phase, we use the vapor pressure measurements by Sydoriak and Roberts.[15] For low

$^3$He concentrations, the ratio of the $^3$He partial pressure $P_X$ to its saturated vapor pressure $P_{sat}$ is proportional to the molar content $X$ in the liquid, $P_X/P_{sat}(T) = B(T)\,X$. We obtain the $B(T)$ dependence by fitting the measured values of $P_X$ vs. $X$ in the small concentration limit for a set of temperatures, and interpolating the results. Since most of $^4$He remains condensed below $T = 2$ K, we can evaluate the content of $^3$He in the film from $X(T) = N_{3He}\,\frac{RT}{P_{sat}(T)\,B(T)\,V_{cell} + N_{4He}RT}$, where $N_{3He}$ and $N_{4He}$ are molar amounts of the helium isotopes in the cell, and $V_{cell}$ is the cell volume.

The lines in Fig. 1 show the attenuation linearly proportional to the concentration of $^3$He in the film, $\alpha_{3He} = \beta X(T)$, where $\beta$ is a multiplier which does not depend either on $^3$He content or temperature. It does, however, depend on the film history and assumes a different value each time the superfluid transition is traversed. To further illustrate the correlation between the attenuation and the $^3$He content of the film, we plot in Fig. 2 the ratio of the two, corrected for $\beta$. The four data sets collapse on the same horizontal in the temperature range between $\sim 0.5$ and 1.1 K.

Data below $\sim 0.5$ K shows deviations from smooth, monotonic behavior, also seen in the measurements in pure $^4$He films. In the range between $\sim 1$ and 0.5 K, the attenuation attributable to $^3$He for all data sets rises somewhat more steeply than the calculated $^3$He density. Expressed in terms of weak temperature dependence of prefactor $\beta$, this correction is no stronger than $\beta \propto T^{-0.2}$.

The observed dependence of the attenuation on temperature indicates that the dominant energy dissipation mechanism is within the film itself. This appears to rule out the evaporation-recondensation mechanism of Bergman[12] as well as energy dissipation through substrate and vapor heat conduction. It is, however, consistent with the dense vortex array model of attenuation.[14] In this latter model, represented schematically in Fig. 3, quantized vortices, trapped by the irregularities at the substrate surface, are deflected in the flow field of the third sound wave due to the Magnus force. The vortex core and the surface dimple then interact with the excitations in the liquid. At low temperatures the vortices are metastable, prevented from annihilating due their strong binding to the microscopic surface defects. The vortex density might be expected to depend on the history of the film's cooling through the superfluid transition. In this model, the effect of the added $^3$He is to introduce additional scattering as the pinned vortices sway periodically in the sound field. If the cross-section of such scattering is independent of temperature, the attenuation can be expected to be proportional to the $^3$He density in the film, with no other temperature dependence.

We are not aware of direct measurements of interaction between vortices in $^4$He and $^3$He impurities. However, there is data available on

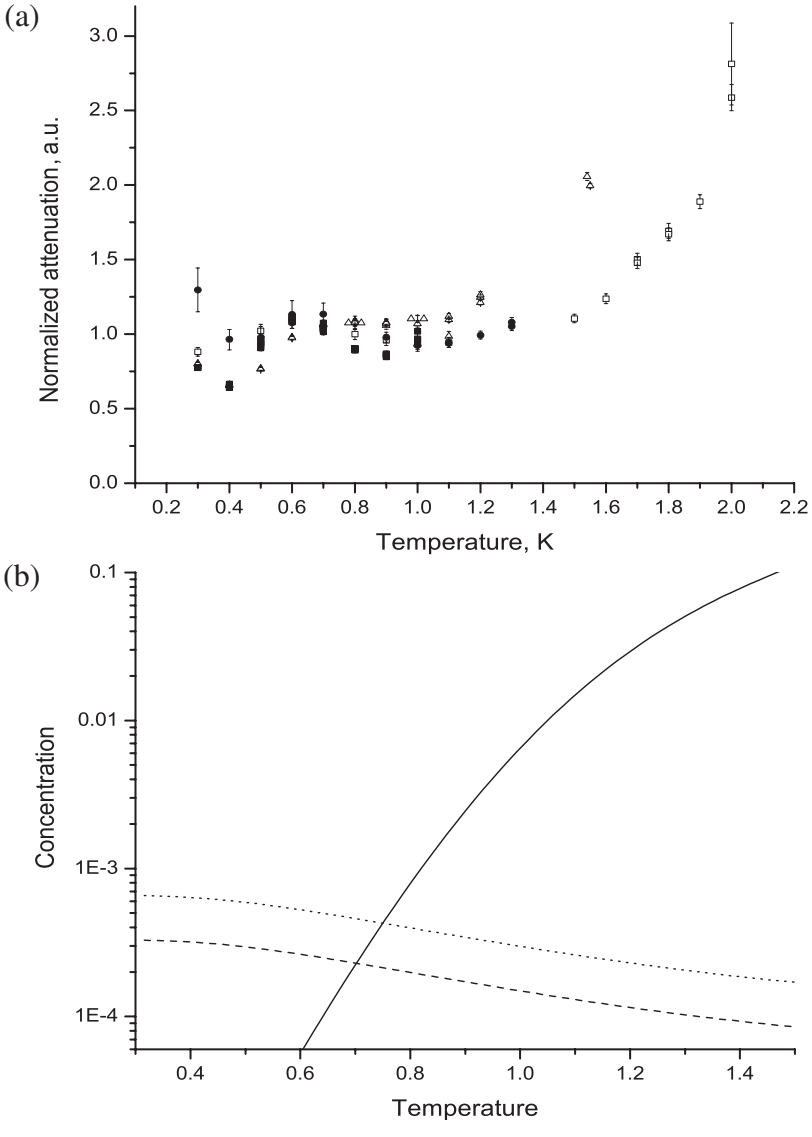


Fig. 2. (a) Attenuation as a function of temperature, normalized to the calculated dependence of $^3$He concentration in the film on temperature and adjusted for a multiplicative factor. Symbols for the attenuation data are the same as in Fig. 1. Horizontal line would correspond to attenuation linear in $^3$He concentration. (b) Calculated normal component fraction (solid line), $^3$He molar concentration for a 330 ppm load (long dash) and 660 ppm load (short dash) as functions of temperature.

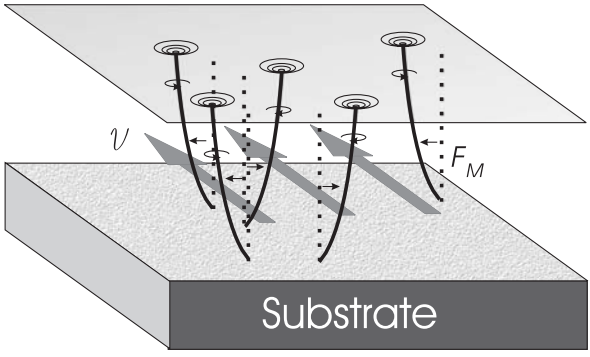


Fig. 3. Schematic depiction of a helium film populated with a dense irregular array of quantized vortices, pinned to the defects at the substrate surface. Vortices are deflected in the oscillating velocity field of third sound by Magnus force. Interaction between the moving vortices and the viscously clamped excitations is dissipative.

interaction of $^3$He atoms with other microscopic entities in superfluid helium. The vortex induced dimple at the surface might be modeled as one part of a moving bubble. The scattering cross-section calculated from measurements[16] of mobility for negative ions in weak solutions of $^3$He in $^4$He shows a weak temperature dependence consistent with a hard sphere interaction potential with a collision radius of 2.1 nm and a Boltzmann thermal distribution of $^3$He momentum. S-wave scattering alone would introduce $\beta \propto T^{1/2}$, which would not be consistent with the temperature dependence we observe. However, below $T \approx 1$ K, resonant scattering is significant, and calculation of its contribution to the attenuation is complicated due to the complex shape of the vortex and the dimple[14].

The calculated concentration of $^3$He is lower than the normal fraction of $^4$He at the attenuation minimum by a factor of $\sim 150$ (see inset in Fig. 2). It remains a mystery to us why the $^3$He atoms should be a more effective dissipative scattering mechanism than the intrinsic normal component. Perhaps the vortex-$^3$He scattering is resonant, with its temperature dependence masked by the dimple shape.

One possible dissipation mechanism would involve the motion of vortices along the substrate surface, with the attachment point jumping from one pinning site to another, or the creation of free vortices via de-pinning.[17] The role of $^3$He then would be to reduce the pinning potential and possibly to create a larger density of free vortices.[18,19] These effects, however, are expected to be strongly dependent on the superfluid flow velocity through

highly non-linear thermal activation. While thermal conductivity and persistent current decay measurements are necessarily made in the film velocity range near onset of nucleation, our measurements involve peak film velocities on the order of $v_{\text{peak}} \approx c_3 \, \Delta d/d \approx 0.3 \, \text{cm/s}$, where $d$ and $\Delta d$ are the typical film thickness and the peak third sound amplitude, respectively. These low velocities and our checks of the linearity of the third sound response seem to rule out any mechanism which involves movement of the vortices along the substrate. Future experiments might check for the effect of surface morphology on pinning by using atomically smooth surfaces (perhaps $\langle 111 \rangle$-oriented silicon wafers) or by pre-treating the substrate in a manner which would greatly reduce the vortex pinning potential, such as pre-plating with an inert gas.

In conclusion, we have presented measurements of the third sound attenuation in thick films of dilute $^3$He:$^4$He solutions. We find that the attenuation seems proportional to the concentration of $^3$He in the film. Since the attenuation function can be changed by a simple multiplicative factor by traversing the lambda point, we suggest that the damping mechanism arises from scattering between the $^3$He atoms and a very dense array of trapped vorticity. Both the density of this trapped vorticity and the specific scattering mechanism remain elusive.

## ACKNOWLEDGMENTS

We would like to acknowledge Mr. Benjamin Hodges for his help in cryostat construction. Two of the authors would also like to thank the other two authors for their nearly infinite patience. This work was supported by the NSF and NASA.

## REFERENCES

1. K. R. Atkins, *Phys. Rev.* **113**, 962 (1959).
2. C. W. F. Everitt, K. R. Atkins, and A. Denenstein, *Phys. Rev. Lett.* **8**, 161 (1962).
3. R. P. Henkel, G. Kukich, and J. D. Reppy, in *Proceedings of the Eleventh Conference on Low Temperature Physics, St. Andrews, Scotland, 1968*, J. F. Allen, D. M. Finlayson, and D. M. McCall, eds., University of St. Andrews Press, St. Andrews, Scotland (1968), p. 178.
4. R. K. Galkiewicz and R. B. Hallock, *Phys. Rev. Lett.* **33**, 1073 (1974).
5. D. T. Ekholm and R. B. Hallock, *Phys. Rev. B* **21**, 3913 (1980).
6. D. Finotello, Y. Y. Yu, and F. M. Gasparini, *Phys. Rev. Lett.* **57**, 843 (1986).
7. K. Penanen, M. Fukuto, I. F. Silvera, and P. S. Pershan, *Phys. Rev. B* **62**, 9641 (2000).
8. F. M. Ellis and H. Luo, *Phys. Rev. B* **39**, 2703 (1989). F. M. Ellis and L. Li, *Phys. Rev. Lett.* **71**, 1577 (1993).
9. J. S. Brooks, F. M. Ellis, and R. B. Hallock, *Phys. Rev. Lett.* **40**, 240 (1978).
10. Stanford Research Systems model SR560 low noise preamplifier.
11. Stanford Research Systems model SR830 DSP lock-in amplifier.
12. D. Bergman, *Phys. Rev.* **188**, 370 (1969).

13. D. Bergman, *Phys. Rev. A* **3**, 2058 (1971).
14. K. Penanen and R. E. Packard, *J. Low Temp. Phys.* **128**, 25 (2002).
15. S. G. Sydoriak and T. R. Roberts, *Phys. Rev.* **118**, 901 (1960).
16. K. W. Schwarz, *Phys. Rev. A* **6**, 1947 (1972).
17. D. A. Browne and S. Doniach, *Phys. Rev. B* **25**, 136 (1982).
18. D. Finotello, Y. Y. Yu, and F. M. Gasparini, *Phys. Rev. Lett.* **57**, 843 (1986).
19. D. T. Ekholm and R. B. Hallock, *Phys. Rev. B* **21**, 3913 (1980).